Journal of Ceramic Processing Research. Vol. 13, No. 1, pp. 71~75 (2012)

J O U R N A L O F
Ceramic Processing Research

Simultaneous synthesis and consolidation of a nanocrystalline $17.14Fe_{0.7}Cr_{0.2}Al_{0.1}$-$Si_3N_4$ composite by pulsed current activated heating

In-Jin Shon[a,*], Song-Lee Du[a], In-Yong Ko[a], Chul-Gyu Song[b], Jung-Mann Doh[c], Jin-Kook Yoon[c] and Sang-Whan Park[c]

[a]*Division of Advanced Materials Engineering and Research Center of Advanced Materials Development, Engineering College, Chonbuk National University, Chonbuk, 561-756, Republic of Korea*

[b]*Division of Electronic Engineering, Engineering College, Chonbuk National University, Chonbuk, 561-756, Republic of Korea*

[c]*Advanced Functional Materials Research Center, Korea Institute of Science and Technology, PO Box 131, Cheongryang, Seoul 130-650, Republic of Korea*

Nanopowders of Fe_3N, Cr, Si and Al powders were fabricated by high-energy ball milling. A high-density nanocrystalline $17.14Fe_{0.7}Cr_{0.2}Al_{0.1}$-$Si_3N_4$ composite was simultaneously synthesized and consolidated by a pulsed current activated sintering (PCAS) method within two minutes from mechanically activated powders of Fe_3N, Cr, Si and Al. The advantage of this process is that it allows very quick densification to near theoretical density and prohibits grain growth in nano-structured materials. The hardness of the composite was about 430 kg/mm^2.

Key words: Nanostructured materials, Sintering, Synthesis, Hardness, Composite materials.

Introduction

Many industrial applications, such as in heating elements, high-tensile components in heat exchangers, or substrates for catalysts applied in catalytic converters and filter systems in automobiles require long-term resistance to oxidation. Iron-aluminium-chromium alloys are applicable as structural materials and coatings for high-temperature applications [1]. Their excellent corrosion resistance is due to the formation of a dense, protective alumina scale. Alumina (α-Al_2O_3 in particular) has a low oxidation rate constant, even at temperatures above 1,000 °C [2]. However, the alloy exhibits a low frictional resistance due to its low hardness. One method to improve hardness is by adding Si_3N_4 to form nanostructured composite materials. Silicon nitride has a high thermal shock resistance, due to its low thermal expansion coefficient, and a good resistance to oxidation when compared to other structural materials [3, 4]. Traditionally, discontinuously reinforced metal matrix composites have been produced by several processes, including powder metallurgy, spray deposition, mechanical alloying, casting, and self-propagating high-temperature synthesis (SHS). A technique that uses SHS developed by Borovinskaya and coworkers [5] in the 1970s, refers to a process in which materials with a sufficiently high heat of formation are synthesized in a combustion wave, which after ignition, spontaneously propagates throughout the reactants and converts them into the product. SHS is extremely attractive, producing a high- purity product due to the volatilization of low boiling point impurities at elevated temperature, and high productivity due to very high reaction rates.

Nanocrystalline materials have received much attention as advanced engineering materials, due to their improved physical and mechanical properties [6, 7]. Nanomaterials typically possess high strength, high hardness, excellent ductility, and toughness. Therefore, increasing attention has been paid to developing potential nanomaterial applications [8]. The grain sizes are much larger in sintered materials than in pre-sintered powders, due to the rapid grain growth that occurs during the conventional sintering processes. Therefore, even though the initial particle size is less than 100 nm, the grain size increases rapidly up to 2 μm or larger during conventional sintering [9]. So, controlling grain growth during sintering is one of the keys to the commercial success of nanostructured materials. Pulsed current activated sintering methods, which can be used to quickly manufacture dense materials within 2 minutes, can control grain growth effectively [10, 11].

The goals of this study were to fabricate a newly-dense nanocrystalline Si_3N_4-reinforced Fe-Cr-Al composite within two minutes from mechanically-activated powders via a pulsed current activated sintering method and to evaluate its hardness and grain size.

Experimental Procedures

Powders of 99.9% pure Fe_3N (< 20 μm, Alfa Co.), 99.5% pure Al (< 45 μm, Alfa Co.), 99.5% pure Si (< 45 μm, Alfa Co.), and 99.8% pure Cr (< 10 μm, Alfa Co.) were used as the starting materials. 4Fe_3N , 3.43Cr, 3 Si, and

*Corresponding author:
Tel : +82-63-270-2381
Fax: +82-63-270-2386
E-mail: ijshon@chonbuk.ac.kr

1.71 Al powder mixtures were milled in a high-energy ball mill (Pulverisette 5 planetary mill) at 250 rpm for 10 h to produce activated nanopowders. Tungsten carbide balls (8.5 mm in diameter) were used in a sealed cylindrical stainless steel vial under an argon atmosphere. The weight ratio of the balls to the powder was 30 : 1. Milling resulted in a significant reduction of the grain size.

After milling, the mixed powders were placed in a graphite die (outside diameter of 45 mm, inside diameter of 20 mm, height of 40 mm) and then introduced into an induced current activated sintering system (Eltek, South Korea), which is shown schematically in Fig. 1. The four major stages in the synthesis are: Stage 1) evacuation of the system, Stage 2) application of a uniaxial pressure, Stage 3) heating of the sample by an induced current, and Stage 4) cooling of the sample. The process was conducted under a vacuum of 40 mtorr (5.33 Pa).

Microstructural information was obtained from product samples that were polished at room temperature. Compositional and microstructural analyses of the products were conducted using X-ray diffraction (XRD) and a field emission scanning electron microscope (FE-SEM) with energy dispersive X-ray analysis (EDAX). The Vickers hardness was measured by performing indentations on the sintered samples at a load of 50 kg and a dwell time of 15 s.

The grain size of Fe-Cr-Al phase were calculated by the formula of Suryanarayana and Grant Norton [12] :

$$B_r\ (B_{crystalline} + B_{strain})\ \cos\theta = k\lambda/L + \eta\sin\theta \qquad (1)$$

where B_r is the full width at half-maximum (FWHM) of the diffraction peak after instrumental correction; $B_{crystalline}$ and B_{strain} are FWHMs caused by the small grain size and internal stress, respectively; k is a constant (k = 0.9); λ is the X-ray radiation wavelength; L and η are the grain size and internal strain, respectively; and θ is the Bragg angle. The parameters B and B_r follow Cauchy's form with the relationship, $B = B_r + B_s$, where B and B_s are FWHMs of the broadened Bragg peaks and the standard sample's Bragg peaks, respectively.

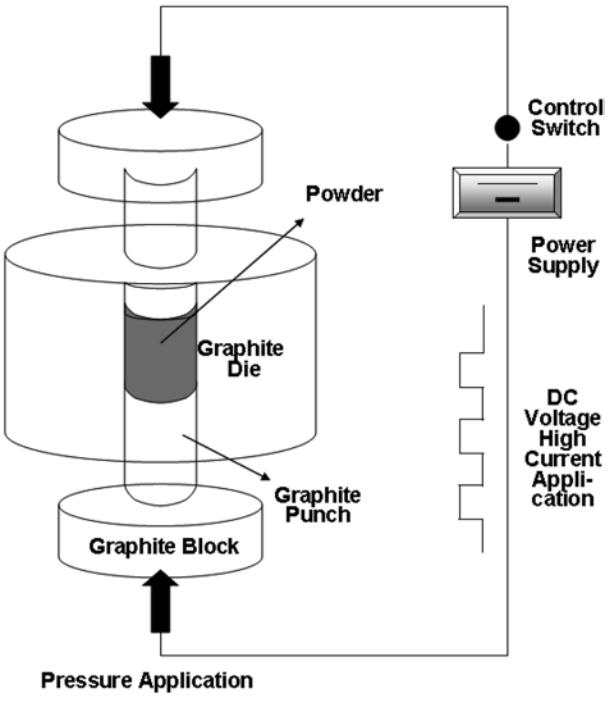

Fig. 1. Schematic diagram of the apparatus for pulsed current activated sintering.

Results and Discussion

The X-ray diffraction results for the high-energy, ball-milled powders are shown in Fig. 2. The Fe_3N, Cr, Si, and Al reactant powders were detected, while the Fe-Cr-Al alloy and Si_3N_4 were not detected. Based on the above results, a mechanical alloy was not formed during the milling. Fig. 3 shows an FE-SEM image and the EDS of the high-energy, ball-milled powders. The powders are very fine with some agglomeration. In the EDS, N, Al, Si, Fe, and Cr are detected.

Fig. 4 shows the variations in the shrinkage displacement and surface temperature of the graphite die with heating time during the processing of the Fe-Cr-Al and Si_3N_4 system. When a pulsed current was applied, the shrinkage displacement slowly increased with temperature up to 900 °C, then increased abruptly to 1040 °C. An X-ray diffraction pattern of a sample heated to 900 °C and 1040 °C is shown in Fig. 5. In Fig. 5(A), the Fe_3N, Cr, Si and Al reactant powders were detected, while in Fig. (B), the Fe-Cr-Al alloy and Si_3N_4 were detected. Based on the above results, the synthesis was formed during the heating. The net reaction can be considered as a combination of the following two reactions:

$$4Fe_3N + 3Si \rightarrow 12Fe + Si_3N_4 \qquad (2)$$

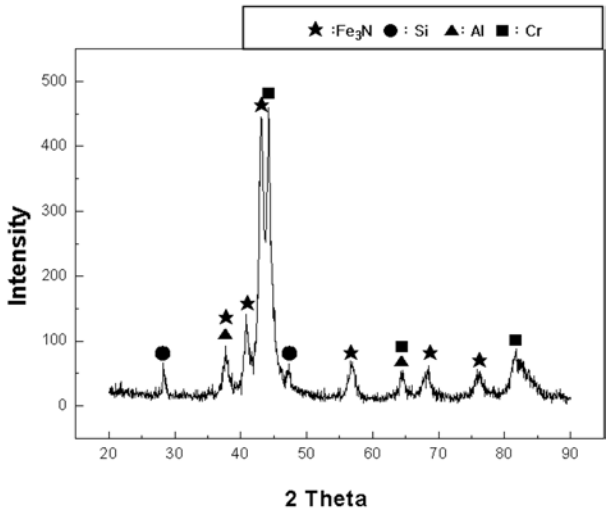

Fig. 2. XRD pattern of the mechanically activated Fe_3N, Cr, Si, and Al powders.

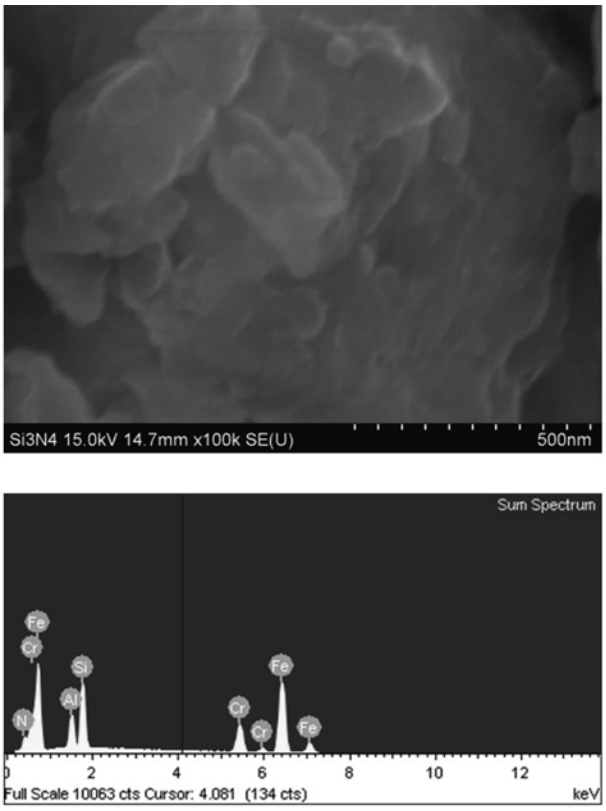

Fig. 3. FE-SEM image and EDS of the mechanically activated Fe_3N, Cr, Si, and Al powders.

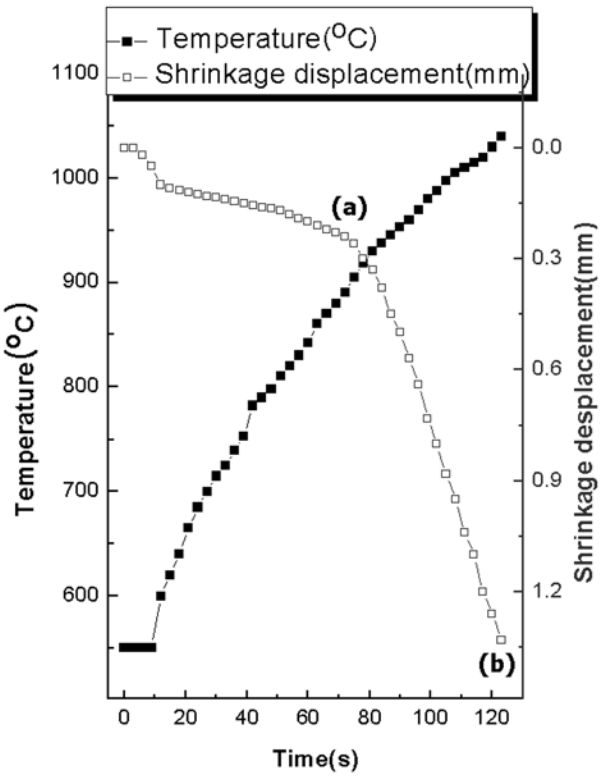

Fig. 4. Variations of the temperature and shrinkage displacement with heating time during pulsed current activated sintering of the 17.14$Fe_{0.7}Cr_{0.2}Al_{0.1}$-Si_3N_4 composite.

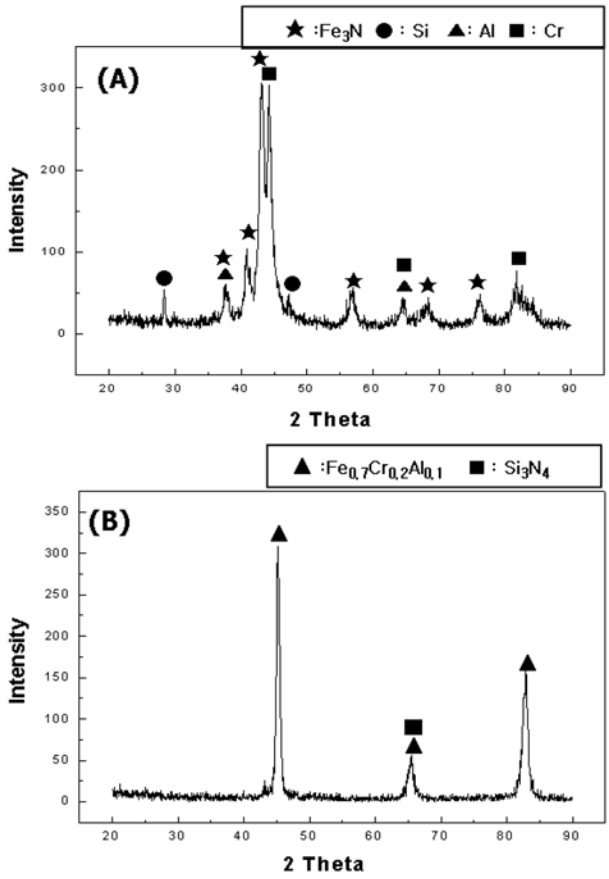

Fig. 5. XRD patterns of the 17.14$Fe_{0.7}Cr_{0.2}Al_{0.1}$-Si_3N_4 system heated to 900 °C (A) and heated to 1040 °C (B).

$$12Fe + 3.43Cr + 1.71Al \rightarrow 17.14Fe_{0.7}Cr_{0.2}Al_{0.1} \quad (3)$$

The abrupt increase in the shrinkage displacement at the ignition temperature in Fig. 4 is due to the increase in density resulting from the change in the molar volume associated with the formation of 17.14$Fe_{0.7}Cr_{0.2}Al_{0.1}$-Si_3N_4 from the reactants (Fe_3N, Cr, Si, and Al) and the consolidation of the product.

Fig. 6 shows the plot of $B_r\cos\theta$ versus $\sin\theta$ to calculate the grain size of $Fe_{0.7}Cr_{0.2}Al_{0.1}$. The structural parameters, i.e. the average grain sizes of $Fe_{0.7}Cr_{0.2}Al_{0.1}$ in the composite sintered from high-energy ball milled powders obtained from the XRD data in Fig. 6 by Suryanarayana and Grant Norton's formula were 35 nm. An FE-SEM image of the 17.14$Fe_{0.7}Cr_{0.2}Al_{0.1}$-Si_3N_4 composite is shown in Fig. 7. The figure shows that the structure consisted of nanophases, and pores were not detected. Thus, nearly a full density of the nanocomposite was obtained. The average grain sizes of the sintered Fe-Cr-Al alloy and Si_3N_4 were not significantly larger than the initial powders, indicating the absence of significant grain growth during sintering. This retention of the grain size is attributed to the high heating rate and the relatively short exposure of the powders to the high temperature. The role of the current in sintering has been the focus of several attempts to explain the

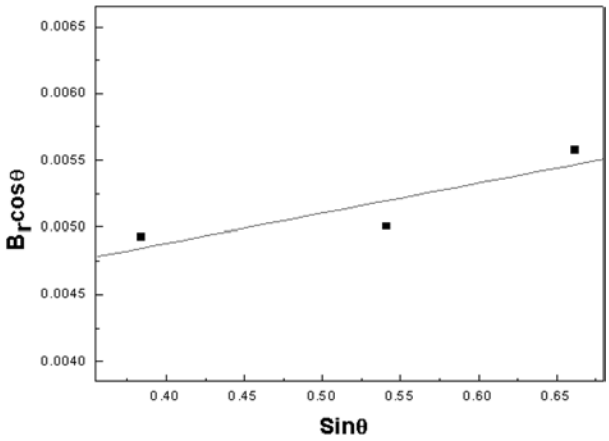

Fig. 6. Plot of Brcosθ versus sinθ of $Fe_{0.7}Cr_{0.2}Al_{0.1}$ in the composite sintered at 1040 °C.

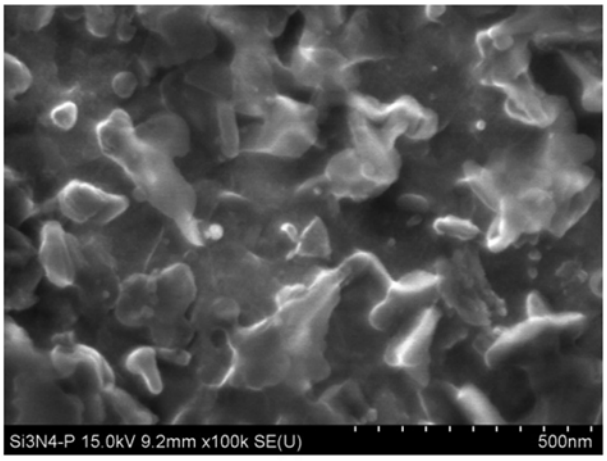

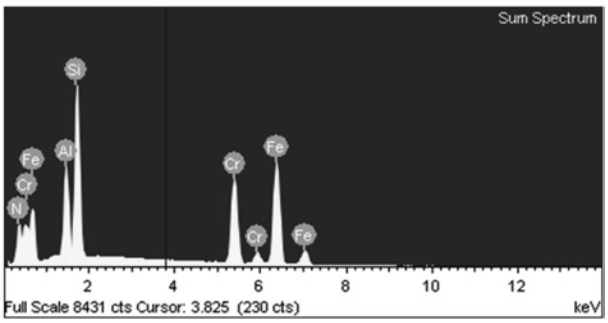

Fig. 7. FE-SEM image of the $17.14Fe_{0.7}Cr_{0.2}Al_{0.1}$-$Si_3N_4$ composite heated to 1040 °C.

observed enhancement of sintering and the improved characteristics of the products. The role played by the current has been interpreted in terms of the rapid heating rate due to Joule heating, the presence of a plasma in pores separating powder particles, and the intrinsic contribution of the current to mass transport [13-16].

Vickers hardness measurements were made on polished sections of the $17.14Fe_{0.7}Cr_{0.2}Al_{0.1}$-$Si_3N_4$ composite using a 50 kg_f load and a 15 s dwell time. The calculated hardness value of the $17.14Fe_{0.7}Cr_{0.2}Al_{0.1}$-$Si_3N_4$ composite

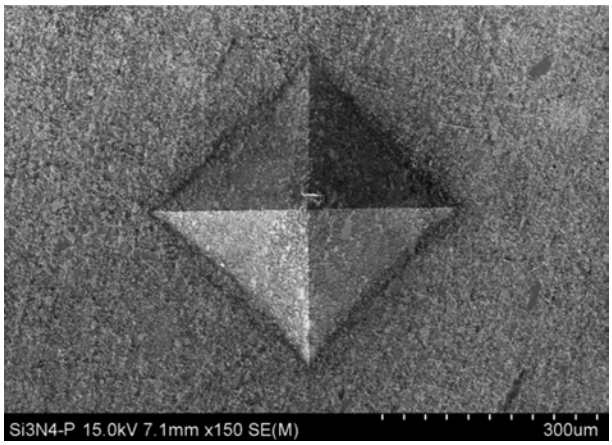

Fig. 8. Vickers hardness indentation of the $17.14Fe_{0.7}Cr_{0.2}Al_{0.1}$-$Si_3N_4$ composite heated to 1040 °C.

was 430 kg/mm^2. Fig. 8 shows a Vickers hardness indentation. Cracks were not produced around the indent. The absence of reported hardness and toughness values for the $17.14Fe_{0.7}Cr_{0.2}Al_{0.1}$-$Si_3N_4$ composite precludes making direct comparisons to the results obtained in this study. However, the hardness and fracture toughness of Si_3N_4 with a grain size of 4.5 μm were previously reported as 1,900 kg/mm^2 and 4.5 $MPa{\cdot}m^{1/2}$, respectively [17, 18]. The hardness of the $17.14Fe_{0.7}Cr_{0.2}Al_{0.1}$-$Si_3N_4$ composite is less than that of monolithic Si_3N_4, but the fracture toughness is greater than that of Si_3N_4 due to the addition of the ductile Fe-Cr-Al alloy.

Conclusions

Nanopowders of Fe_3N, Cr, Si, and Al powders were fabricated by high-energy ball milling. Using the pulsed current activated sintering method, we accomplished simultaneous synthesis and densification of a nanostructured $17.14Fe_{0.7}Cr_{0.2}Al_{0.1}$-$Si_3N_4$ composite from mechanically activated powders. Complete densification could be achieved within a processing time of two minutes under an applied pressure of 80 MPa and a pulsed current. The average grain sizes of the Fe-Cr-Al alloy prepared by PCAS were lower than 100 nm. The average obtained hardness value was 430 kg/mm^2.

Acknowledgements

This work was supported by the New & Renewable Energy R&D Program (2009T00100316) of the Ministry of Knowledge Economy, Republic of Korea.

References

1. J. Klower, Materials and Corrosion 47 (1996) 685-694.
2. P. Kofstad, "High temperature corrosion", Elsevier Appl. Sci. Publ., London, New York, 1988.
3. W. Dressler and R. Riedel, Int. J. Refract. Met. Hard

Mater. 15 (1997) 13-18.
4. Simone Pereira Taguchi, Sebastião Ribeiro, J. Materials Processing Technology 147 (2004) 336-342.
5. I.P. Borovinskaya, A.G. Merzhanov, N.P. Novikov and A.K. Filonenko, Combust. Explos. Shock Waves 10 (1974) 2-10.
6. M.S. El-Eskandarany, J. Alloys & Compounds 305 (2000) 225-238.
7. L. Fu, L.H. Cao and Y.S. Fan, Scripta Materialia, 44 (2001) 1061-1068.
8. S. Berger, R. Porat and R. Rosen, Progress in Materials Science, 42 (1997) 311-320.
9. J. Jung and S. Kang, Scripta Materialia 56 (2007) 561-564.
10. H.C. Kim, I.J. Shon, I.J. Jeong, I.Y. Ko, J.K. Yoon and J.M. Doh, Metals and Materials International 13 (2007) 39-46.
11. H.C. Kim, I.J. Shon, I.K. Jeong and I.Y. Ko, Metals and Materials International 12 (2006) 393-399.
12. C. Suryanarayana and M. Grant Norton, X-ray Diffraction A Practical Approach, Plenum Press, New York and London.
13. Z. Shen, M. Johnsson, Z. Zhao and M. Nygren, *J. Am. Ceram. Soc.,* 85 (2002) 1921-27.
14. J.E. Garay, U. Anselmi-Tamburini, Z.A. Munir, S.C. Glade and K.P. Asoka, *Appl. Phys. Lett.*, 85 (2004) 573-575.
15. J.R. Friedman, J.E. Garay, U. Anselmi-Tamburini and Z.A. Munir, *Intermetallics*, 12 (2004) 589-597.
16. J.E. Garay, U. Anselmi-Tamburini and Z.A. Munir, *Acta. Mater.* 51 (2003) 4487-4495.
17. H.L. Wang and M.H. Hon, Ceramics International, 25 (1999) 267-271.
18. A. Vuckovic, S. Boskovic, B. Matovic, M. Vlajic and V. Krstic, Ceramics International 32 (2006) 303-307.